# APPENDIX B

# BACKGROUND ALGORITHMS AND IMAGE ANALYSIS EXAMPLES OF VIDEO-BASED LUMINANCE MAPPING SYSTEM

## B.1 DETERMINING DAYLIGHTING PARAMETERS

### B.1.1 Video Image Capture and Conversions

To capture the 180° full-field images of a luminous environment, the video camera assembly is located vertically or horizontally at reference points inside scale models. The locations of the camera assembly may be determined by considering designed task locations. After an image is digitized, its aspect ratio has to be corrected by Aspect Ratio Correction Module before determining the geometric and photometric parameters. The captured image has a width-to-height ratio of 1:1.25 in pixel-to-pixel distance which is calculated by 480/3 (= 160) divided by 512/4 (= 128). The numbers 3 and 4 indicate the height-to-width ratio of the TV monitor screen. When the uncorrected image of a circular target is digitized and displayed on the computer monitor (VGA color, 640x480 pixels) with width-to-height ratio of 1:1 in pixel-to-pixel distance, the circular target is displayed as an ellipse elongated vertically.

The next step is to convert equidistant projection images into orthographic projection images by Orthographic Conversion Module to determine the Configuration Factors and solid angles of daylight surface sources. As shown in Figure B.1, the incident angle θ of a pixel on the equidistant projection image is calculated using the radial distance of the pixel from the center point by Equation B.1.

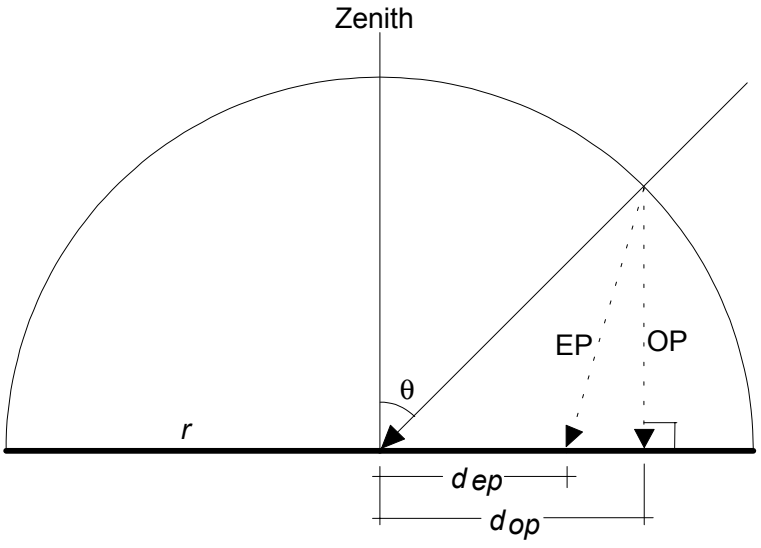


Figure B.1 Equidistant and Orthographic Projections

$$\theta = \frac{dep}{r} \times \frac{\pi}{2} \tag{B.1}$$

where $\theta$ = incident angle (radians)
$d_{ep}$ = distance from the center in equidistant projection
r = radius

Then, a new radial distance $d_{op}$ on the orthographic projection image is given by Equation B.2.

$$d_{op} = r \sin \theta \tag{B.2}$$

Figure B.2 shows a scale model with vertical windows and clerestories. Figure B.3 shows the equidistant projection image captured by the vertically located (i.e., shooting upward) camera assembly at the center point of the room. The orthographic projection image converted from the equidistant projection image is shown in Figure B.4. It shows the geometric expansions of the objects in the center portion and compressions near the edge. The original equidistant projection image has an advantage over an orthographic projection image in recording the distribution of the sky luminances as a function of zenith and azimuth angles because it does not produce geometric compressions near the horizon. However, in order to determine the geometric and photometric parameters of daylighting surface sources, orthographic projection images must be used as will be discussed in the next sections.

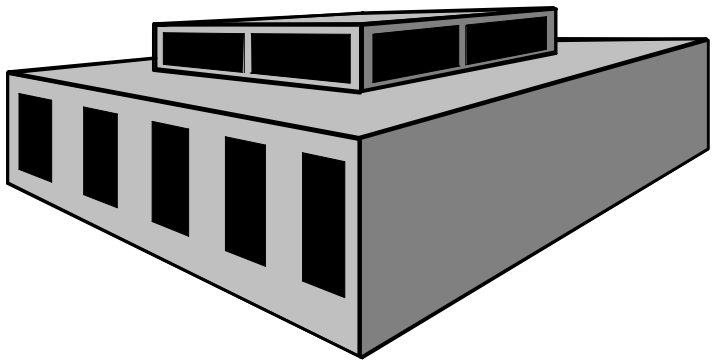

Figure B.2 Outside View of Scale Model

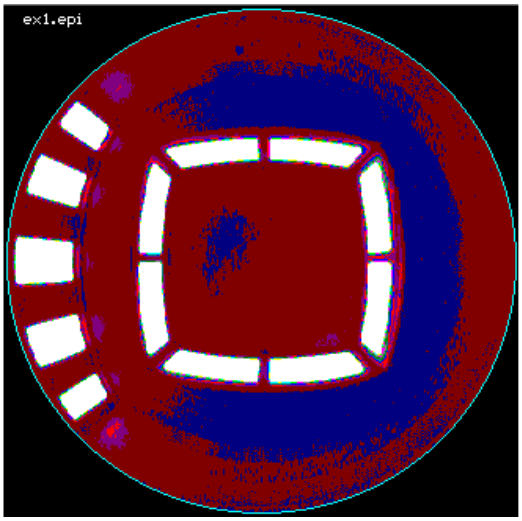


Figure B.3 Equidistant Projection Image of Vertical Windows and Clerestories

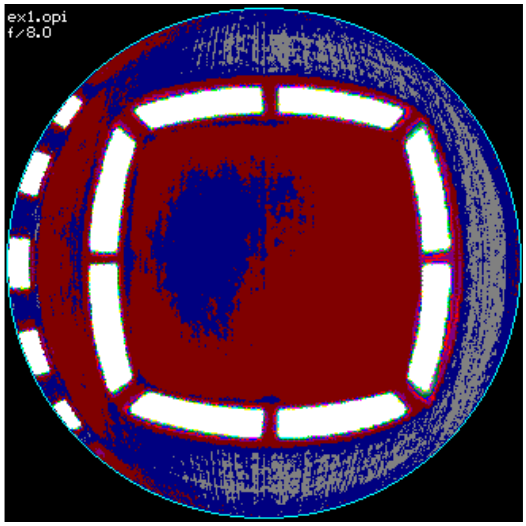


Figure B.4 Orthographic Projection Image Converted from Equidistant Projection Image

### B.1.2 Determining Geometric Parameters

The current system can be used to determine Sky Factors (SF) of windows or skylights at given points inside a building. It also can be used to determine Configuration Factors (CF) of interior surfaces.

The Sky Factor at a point on a given plane, which is a pure geometric ratio, is defined as $1/\pi$ of the area orthographically projected on the plane from the surface intercepted on a sphere of unit radius with its center at the point by a cone having the point as its apex and the contour of that part of the sky visible from the point as its base. (Hopkinson et al. 1966, p. 70). The concept of Sky Factor (SF) is similar to that of Sky Component (SC) in the simple daylight factor method. However, there is a clear difference between them. The Sky Component (SC) of Daylight Factor (DF), which is a photometric ratio, is the measure of direct daylight under all conditions other than uniform sky and unglazed openings, which are the basis for SF calculations, and is therefore the usual measure of the direct daylight (Hopkinson et al. 1966, p. 70).

The Configuration Factor (CF) is the generic term and is used preferably when referring to light which reaches the reference point other than directly from the sky, e.g. after reflection from some exterior or interior surface. (Hopkinson et al. 1966, p. 71). This generic term was used throughout the subsequent procedures to determine the geometric parameters of surface sources of light.

As shown in Figure B.5, the direct illuminance at point P on a horizontal surface T illuminated by a diffuse surface source of S [m²] having a uniform luminance L [cd/m²] is given by Equation B.3

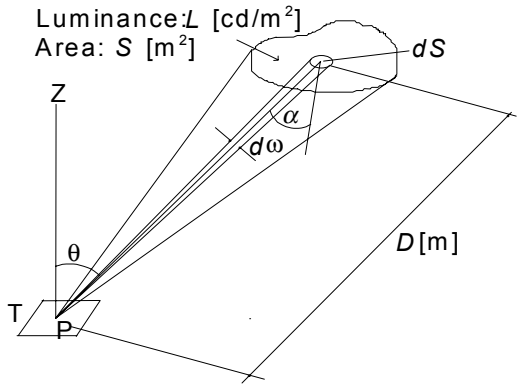


Figure B.5 Geometric Relationship between a Surface Source and a Reference Point

$$E_p = L\int_S \frac{\cos\alpha\cos\theta}{D^2} dS \tag{B.3}$$

The assumption that the surface source has a uniform luminance permits the luminance L [cd/m²] to be replaced by luminance emittance M [rlx or lm/m²] to yield Equation B.4, because M = π L under this assumption.

$$E_p = M\int_S \frac{\cos\alpha\cos\theta}{\pi D^2} dS \tag{B.4}$$

In Equations B.3 and B.4, L and M represent the quantities of light, while the integrand includes purely geometric properties such as angles, distance and area. The Configuration Factor (CF) is expressed as Equation B.5 and explains the geometric relationship between the light source and the receiving point.

$$CF = \int_S \frac{\cos\alpha\cos\theta}{\pi D^2} dS \tag{B.5}$$

If the solid angle dω [steradians], where dω = dS cosα / $D^2$, subtended at the point P due to dS is substituted into Equation B.5, then Equation B.6 can be obtained.

$$CF = \int_\omega \frac{\cos\theta}{\pi} d\omega \tag{B.6}$$

where ω = the solid angle subtended at the point P due to the entire area S [m²].

Finally, the relationship for illuminance at the point P can be expressed as Equation B.7.

$$E_p = \pi L(CF) = M(CF) \tag{B.7}$$

However, Equations B.5 and B.6 have no closed form solutions except for extremely simple geometries. An alternative approach to the determination of CF is a graphical method which is well known as the solid angle projection principle. As shown in Figure B.6, a hemisphere with a unit radius is drawn around the reference point P.

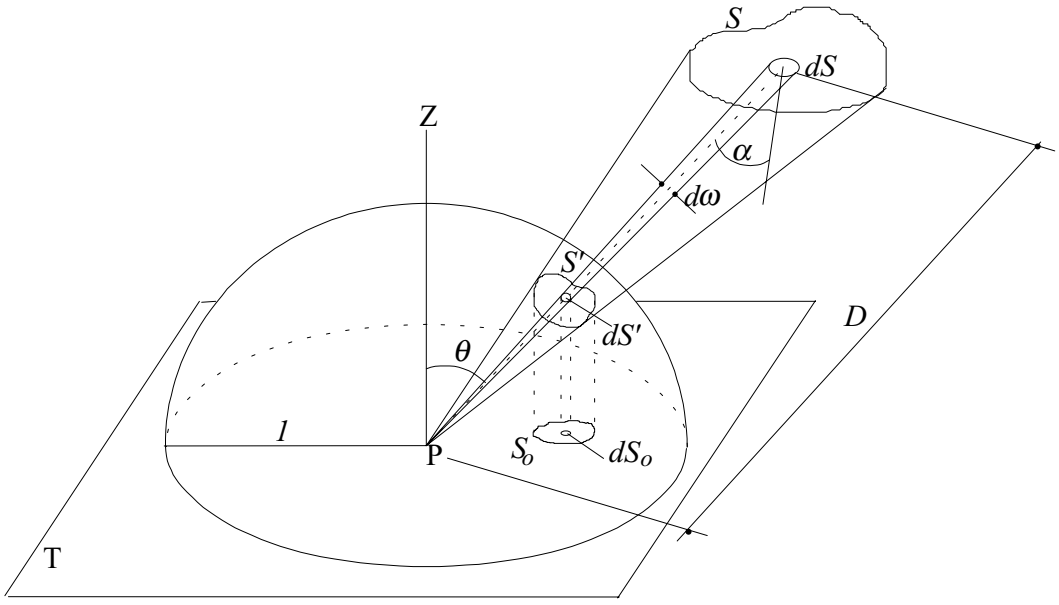


Figure B.6 Orthographic Projection of Solid Angle

Then, the solid angle subtended at the point P due to the infinitesimal area dS is given by Equation B.8.

$$d\omega = \frac{dS\cos\alpha}{D^2} = \frac{dS'}{1^2} \tag{B.8}$$

Since the area of $dS_o$ on the plane T, which is the orthographically projected image of dS', is equal to dS' cosθ, the infinitesimal solid angle dω can be expressed as Equation B.9.

$$d\omega = \frac{dS_o}{\cos\theta} \tag{B.9}$$

By substituting Equation B.9 into Equation B.6, the CF can be obtained by Equation B.10.

$$CF = \int_{S_o} \frac{1}{\pi} dS_o = \frac{S_o}{\pi} \tag{B.10}$$

Equation B.10 indicates that the CF of the surface source of S is given by the area of $S_o$ divided by the area of the unit circle drawn on the plane T. Again, to determine $S_o$ by a pure computational method may be easy only with simple geometries such as rectangular, triangular or circular surface sources. However, this equation is easy to solve for any geometries of daylight surface sources if they are captured and visualized as orthographic projection images by a full-field projection video camera, such as SERI-LM2 or the one developed in this research.

In digitized images, the area of a region can be determined by counting the number of pixels in the region. In this case, $S_o$ can be determined by counting the number of pixels in a projected daylight surface source, while the unit circle area $\pi$ is represented by the total number of pixels in the circle. Therefore, Equation B.10 can be converted again into Equation B.11.

$$CF = \frac{n}{N} \tag{B.11}$$

where n = number of pixels in orthographic projection image of surface source
N = total number of pixels in projected circle

In the current full-field luminance mapping system, the circle contains a total of 82,429 pixels. To count the number of pixels in the projected images of daylighting surface sources, the current system utilizes two image segmentation algorithms. Segmentation is the process that subdivides an image into its constituent parts or objects. Segmentation algorithms are generally based on one of two basic properties of gray-level values: discontinuity and similarity. With the first property, an image can be partitioned based on abrupt changes in gray level. The main approaches using the second property are based on thresholding, region growing, and region splitting and merging (Gonzalez and Wintz 1987, p. 331).

The current image analysis program adopted the thresholding and the region growing algorithms. The thresholding algorithm is mainly used to determine the CF values of openings with relatively non-uniform luminances. The region growing algorithm is suitable for geometrically continuous objects with relatively uniform luminances. To use the thresholding algorithm in determining the CF of a surface source of

interest, the user moves a pointing device to draw a rectangular boundary around the surface source and defines lower and upper thresholds by visually examining the pixel colors assigned to the surface source. Finally, the image processing program scans the pixels within the boundary and counts the number of pixels having the gray levels which pass the thresholds.

As an alternative, to use the region growing algorithm, the user draws a rectangular boundary around the surface source and picks a seed pixel within the area of interest. Then, the image processing program scans every neighboring pixel within the defined boundary and counts the number of pixels if their gray levels do not abruptly change and at least one of their eight neighboring pixels has been previously included.

### B.1.3 Determining Photometric Parameters

The pixel intensities recorded by the current luminance mapping system have integer values between 0 and 255 which represent 256 gray levels at each of seven aperture settings of the fisheye lens. These values can be converted to the actual luminances by applying the calibration curves. First, the off-axis luminance transfer function curves are used to correct the intensities of pixels located off axis. Then, the on-axis system response function curves are used to determine the actual luminances of infinitesimal areas represented by the pixels in the projected image. The illuminance [lux or lm/m²] at the camera position can be calculated by manipulating the pixel luminance values by the following procedures.

The solid angle subtended at the camera position P associated with the entire hemisphere is $2\pi$ steradians and its orthographically projected area on the unit circle is $\pi$. Therefore, an infinitesimal solid angle $d\omega$ on the surface of the unit hemisphere represented by each pixel in the unit circle is given by Equation B.12

$$d\omega = \frac{\pi}{N} \times \frac{1}{\cos\,\theta} \tag{B.12}$$

In this case, the angle $\theta$ is the incident angle of the center light ray emitted by the infinitesimal area. Figure B.7 shows the solid angles represented by pixels with different incident angles (i.e., zenith angles) in the current system.

Since the solid angle $d\omega$ and luminance dL [cd/m²] of an infinitesimal area is known, the illuminance due to the infinitesimal area can be calculated by Equation B.13

$$dE = dL \cos\theta \, d\omega \tag{B.13}$$

By substituting Equation B.12 into Equation B.13, dE can be expressed as

$$dE = dL \frac{\pi}{N} \tag{B.14}$$

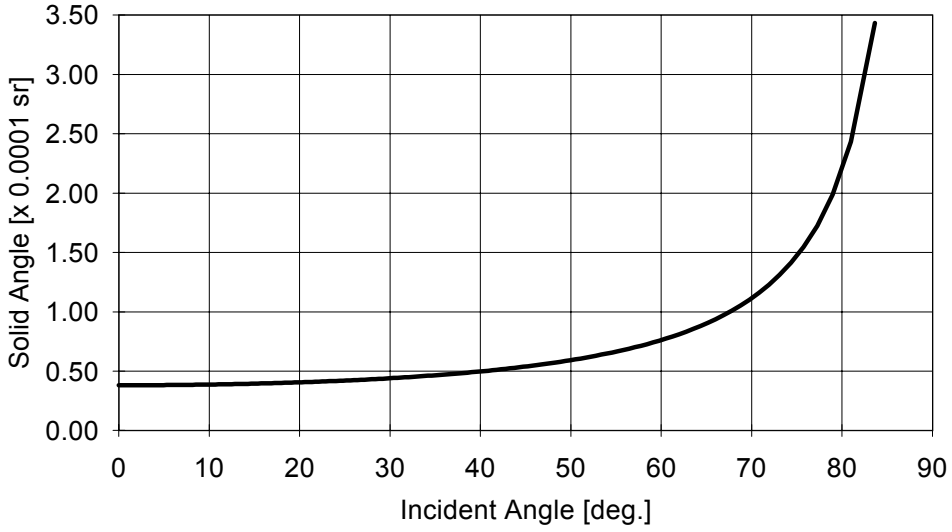


Figure B.7 Solid Angles of Pixels as a Function of Incident Angles

If dE and dL are replaced respectively by $E_i$ and $L_i$ for the discrete ith pixel in the orthographic projection image, the illuminance at the point P due to a surface source with non-uniform luminances represented by n pixels in the orthographic projection image is given by Equation B.15.

$$E_p = \sum_{i=1}^{n} E_i = \frac{\pi}{N} \sum_{i=1}^{n} L_i \tag{B.15}$$

Equation B.15 demonstrates an advantage of the full-field luminance mapping system over conventional photometric measurements in analyzing the effects of architectural design options. The merit of using this method is that the net effect of individual daylight sources on the illuminance level at the reference point can be easily

tested independent of others. Using this method, for example, the designer can examine the net effect (direct component) of each of different window design options and can determine which area of interior surfaces has a major impact (interreflected component) on the illuminance levels at the reference points. If the surface source has a uniform luminance L such as a uniform sky, Equation B.15 can be simplified as Equation B.16.

$$E_p = \frac{\pi}{N}\sum_{i=1}^{n} L = \pi L \frac{n}{N} = \pi L(CF) \tag{B.16}$$

Since the result is the same as Equation B.7, Equation B.16 may be another way of proving that the Configuration Factor (CF) in the orthographic projection image is n/N. Finally, the illuminance at the point P due to the entire hemisphere with non-uniform luminances is determined by Equation B.17. This equation is the basis for the Luminance Index (LI) development in Chapter 7.

$$E_p = \pi\left(\frac{1}{N}\sum_{i=1}^{N} L_i\right) = \pi\overline{L} \tag{B.17}$$

where $\overline{L}$ = average field luminance.

## B.2 EXAMPLES OF DIGITAL IMAGE ANALYSIS

Figure B.8 shows the interior image of a room with vertical windows and a waffle skylight system captured at f/11. The outdoor horizontal illuminance ($E_{do}$) was measured 6390 lux. The indoor horizontal illuminances at the center point of the room which were measured by a photometric sensor and determined by the current system were 1410 lux and 1440 lux, respectively. As shown in Figure B.9, the image processing program calculated the overall Sky Factor (SF) of the openings to be 0.2513 (25.1%). The illuminance from the unobstructed sky and that reflected by the room surfaces including the surfaces of the skylight structure were 1115 lux and 325 lux, respectively.

Figure B.10 demonstrates the thresholding algorithm and the region growing algorithm applied to openings A and B, respectively, to determine the geometric and photometric parameters of these two specific openings. The SF values of openings A and B were 0.0323 and 0.0123, respectively, at the camera location. The average luminances were 1036 cd/m² and 1552 cd/m², respectively. Finally, the illuminances from these two openings were 105 lux and 60 lux, respectively.

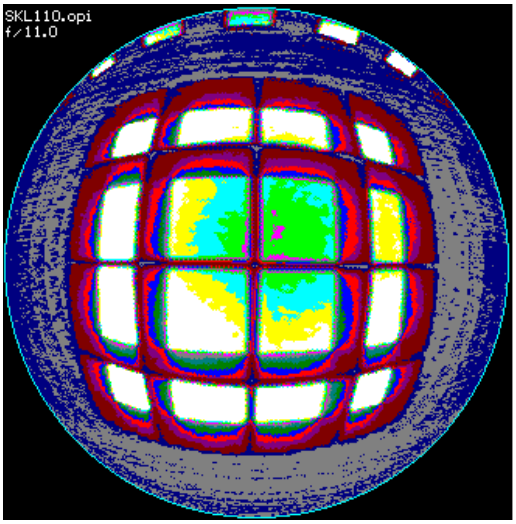


Figure B.8 Orthographic Projection Image of Vertical Windows and Waffle Skylight
(f/11, $E_{do}$ = 6390 lux, $E_p$ = 1440 lux)

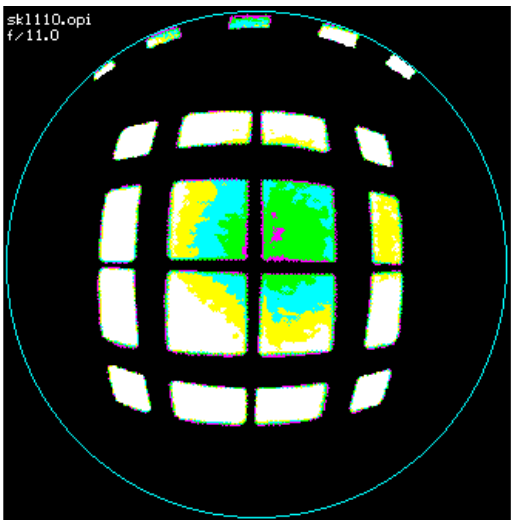


Figure B.9 Image of Segmented Vertical Windows and Waffle Skylight to Determine Overall Sky Factor (f/11, $E_p$ = 1115 lux, SF = 0.2513)

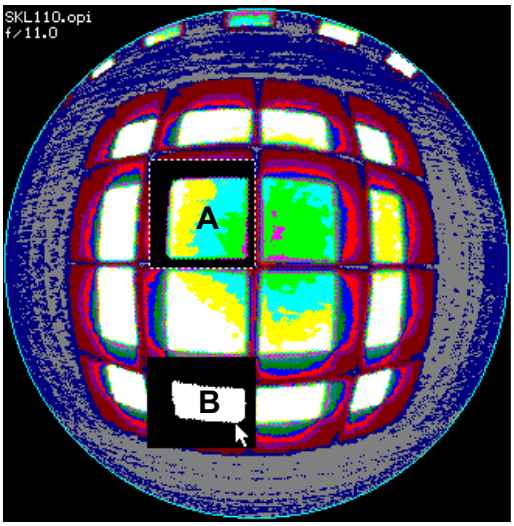


Figure B.10 Image of Individual Openings of Waffle Skylight Analyzed by Thresholding (A) and Region Growing (B) Algorithms

The next two figures demonstrate another possible application of the current system in determining the illuminance and the SF of the unobstructed sky at outdoor locations or in atrium spaces with irregular shape floor plans. Figure B.11 shows an image captured at the camera location surrounded by scale models to simulate those situations inside the sky simulator. The illuminance from the unobstructed sky and that reflected by the building surfaces were 234 lux and 90 lux, respectively. Figure B.12 shows the unobstructed sky portion processed by thresholding algorithm. A total of 28128 pixels were counted for the sky area, yielding the SF of 0.3412 (34.1%). Figures B.13 through B.16 show other image analysis methods with full screen images of the current video-based luminance mapping system.

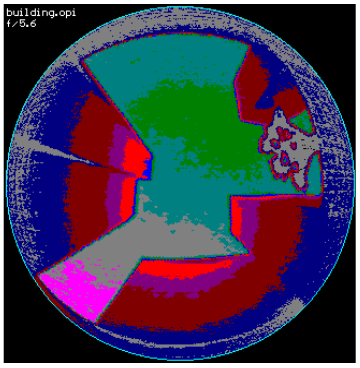


Figure B.11 Image of Irregular Shape Sky Seen through Building Structures and a Tree

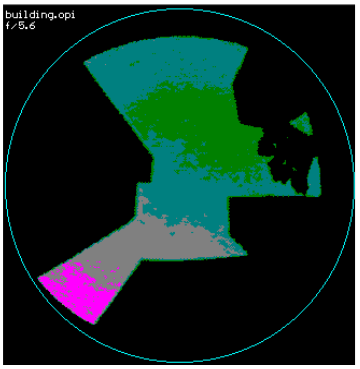


Figure B.12 Image of Segmented Unobstructed Sky Area (f/5.6, n = 28128, SF = 0.3412)

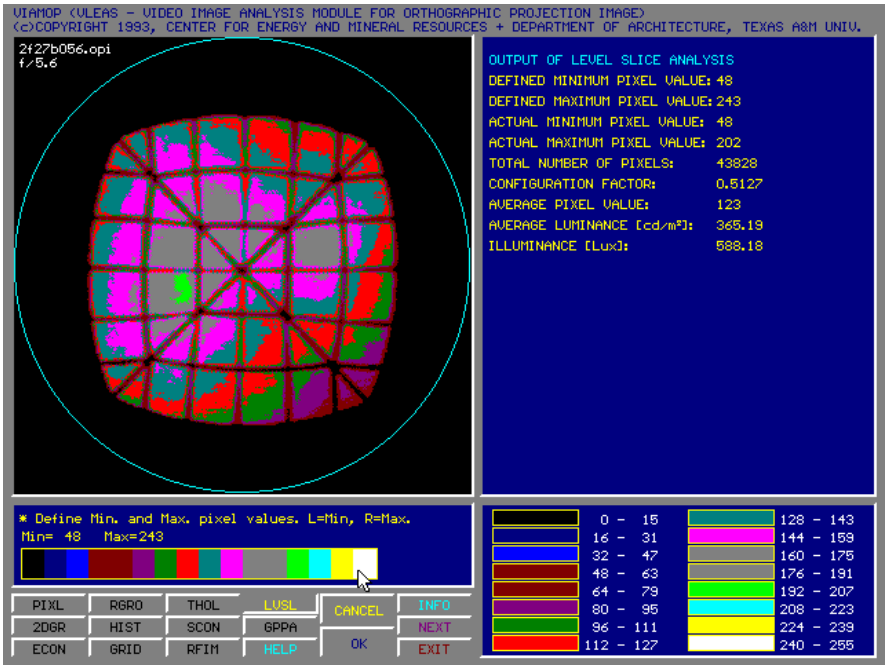


Figure B.13 Level Slice Analysis with Image

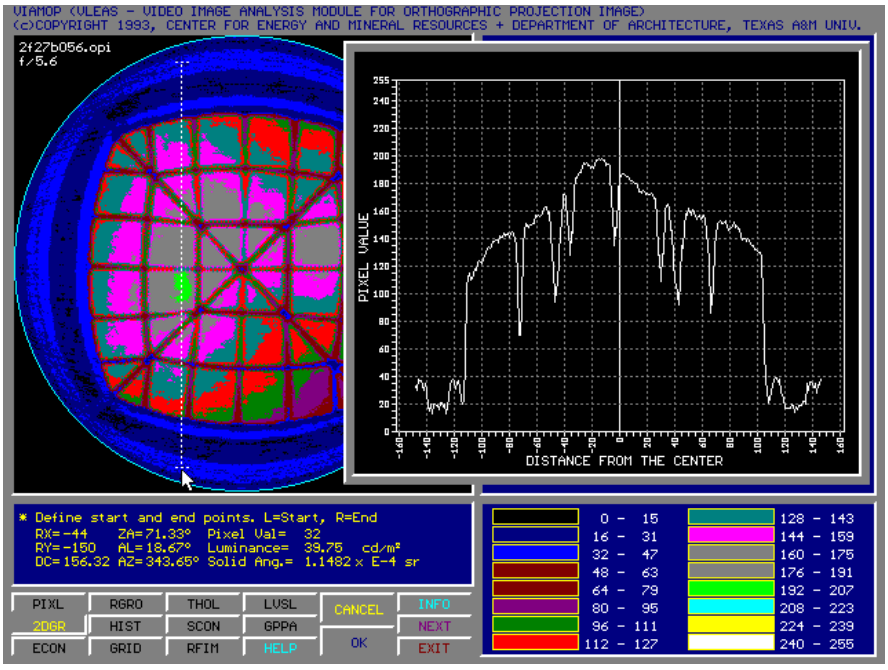


Figure B.14 Luminance Cross Section with Image

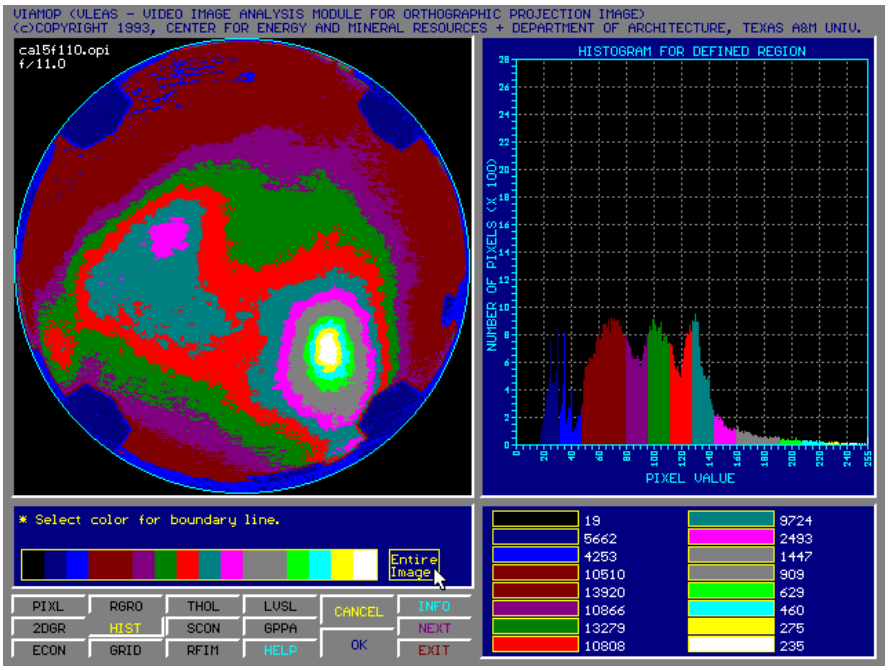


Figure B.15 Luminance Histogram with Image

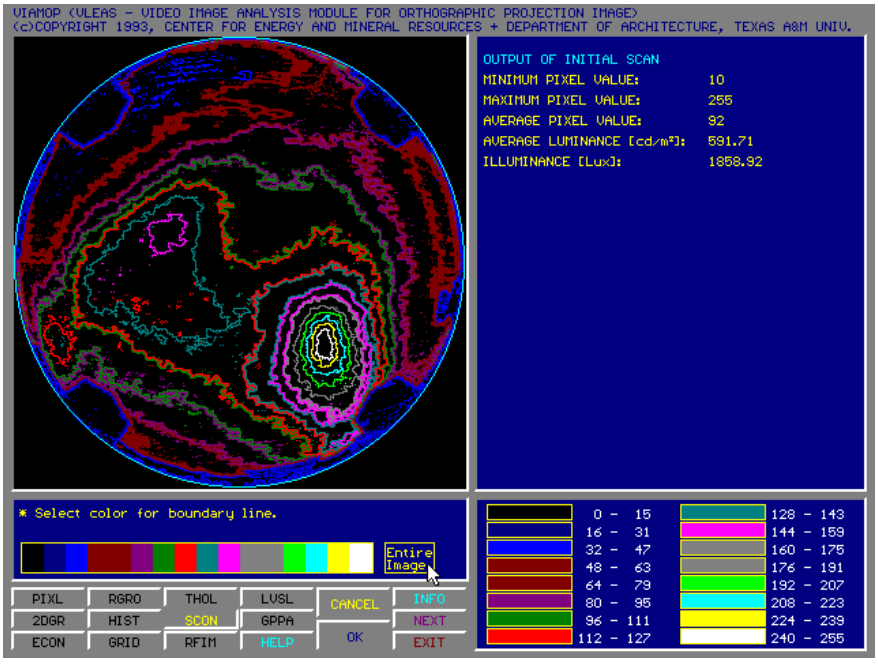


Figure B.16 On-Screen Contour Plots of Image